Pergamon

Journal of Structural Geology, Vol. 18, No. 6, pp. 765 to 776, 1996

0191-8141/96 $15.00+0.00

PII: S0191-8141(96)00006-5

Misalignment of quartz c-axis fabrics and lineations due to oblique final strain increments in the Ruby Mountains core complex, Nevada

TYLER MacCREADY*

Department of Geology and Geophysics, University of Wyoming, Laramie, WY 82071-3006, U.S.A.

(*Received* 1 *November* 1993; *accepted in revised form* 16 *January* 1996)

Abstract—To interpret c-axis stereonet patterns of deformed quartz the patterns must be viewed in the XZ strain plane, which is usually assumed to contain the elongation lineation. This study describes several c-axis patterns from a region of complex, amphibolite facies deformation in the northern Ruby Mountains where the late XZ plane is oblique to most of the lineations. Without the lineation as a guide, the proper orientation for interpretation of each pattern is determined by rotating the c-axis data around the normal to the foliation until the c-axes within the foliation plane lie at the center of the stereonet. This new view is inferred to be the XZ plane for the final increments of strain. The rotation produces an internal symmetry in the patterns. In addition, the rotated views across the area show a more consistent geographic orientation than the lineations. This geographic orientation is aligned with strain in a mylonitic shear zone which represents the latest macroscopic evidence for plastic strain along the edge of the study area.

The complete reorientation of the quartz textures during the final strain increments implies that they record very little of the finite strain history. Quartz is the only mineral recrystallized during the late strain thereby providing insight into the geometry of strain increments that cannot be determined from other minerals. Copyright © 1996 Elsevier Science Ltd

INTRODUCTION

The use of quartz c-axis patterns in structural analysis in based on the principle that the geometry of the patterns relates to the geometry of strain. Experimental studies indicate that deforming quartz grains attain preferred c-axis orientations by preferably orienting crystallographic slip planes (Tullis 1977, Ralser *et al.* 1991, Gleason *et al.* 1993). The majority of numerical, experimental, and field studies indicate that slip tends to occur parallel to the <a> crystallographic axes (Tullis 1977, Lister & Hobbs 1980, Malavieille & Etchecopar 1981, Schmid & Casey 1986, Etchecopar & Vasseur 1987, Lloyd & Freeman 1994). The interactions of multiple grains, slip systems and dynamic recrystallization are not yet fully understood (Wenk & Christie 1991), but in naturally deformed quartzites there is a tendency for c-axes within the foliation plane to be perpendicular to the finite extension direction defined by the elongation lineation (e.g. Schmid & Casey 1986, Law 1990). In some studies, c-axis patterns have been observed which do not show this geometric relation (Simpson 1980, Gapais & Barbarin 1986, Klaper 1988, Melka *et al.* 1992, Peterson & Robinson 1993). When this occurs, there are a number of possible reasons for the discrepancy (Lister & Williams 1979, Brunel 1980): (1) the final strain increment may not be consistent with the finite strain thereby reorienting the quartz texture, (2) an older inherited texture may have influenced the final c-axis distribution, (3) some slip may have occurred parallel to the <c> crystallographic axes. Usually it is not possible to determine the cause for the discrepancy because of a lack of geometric constraints. In this study, a relatively complete knowledge of the geochronology and strain geometries allow the conclusion that the quartz textures are aligned by a final strain increment oblique to the finite strain.

The results of this study imply that quartz textures developed at amphibolite facies conditions may have little relation to the finite strain history. The role of recrystallization is examined to see how the quartz texture could reorient to the latest strain direction while the accessory minerals defining the lineation and foliation maintain their original orientations.

GEOLOGIC SETTING

Samples for this study were collected from an area of complex, amphibolite grade deformation in the Ruby Mountains metamorphic core complex, Nevada (Fig. 1). Within the study area there are two structural levels which together make up the footwall beneath a brittle detachment system. The upper level of the footwall is a subhorizontal to west-dipping mylonitic shear zone about one kilometer thick exposed in the west and north. The mylonitic rocks contain a well developed, W–NW-trending lineation defined by elongate aggregates of feldspar and oriented sillimanite needles (Fig. 2). The lower level, referred to as the infrastructure (Howard 1980, Snoke 1980, following terminology of Armstrong & Hansen 1966), is also subhorizontally foliated, but the quartzites are coarser grained than in the mylonitic shear zone and they contain a N–NE-

*Present address: Department of Earth Sciences, Monash University, Clayton, Victoria 3168, Australia.

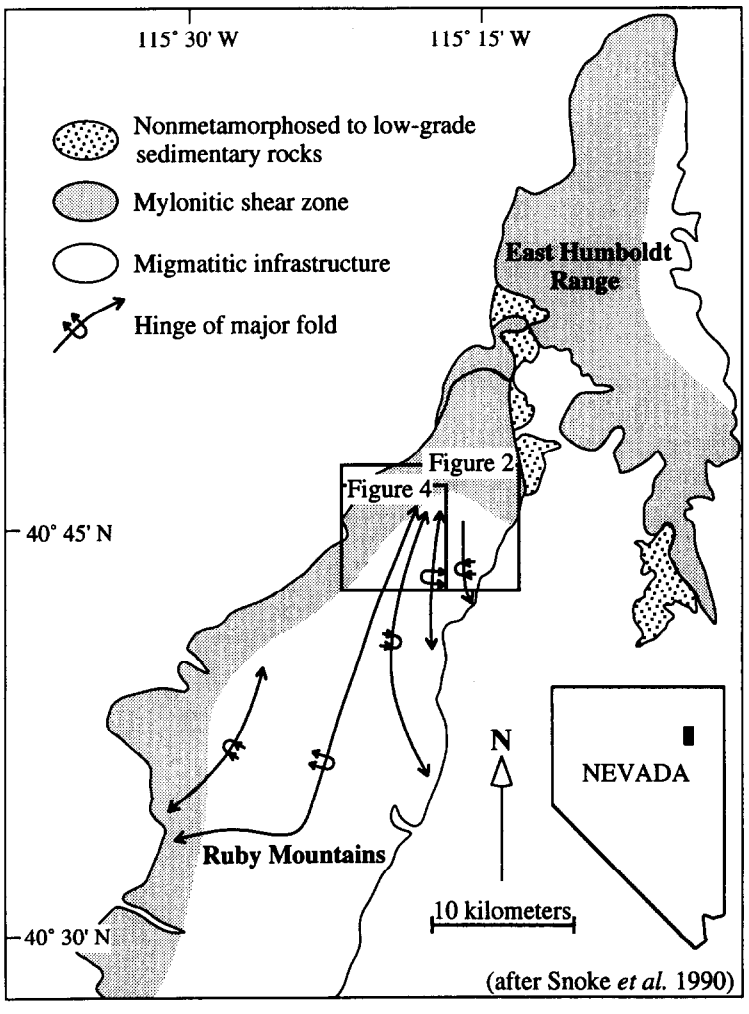

Fig. 1. Structural map of the northern Ruby Mountains and East Humboldt Range.

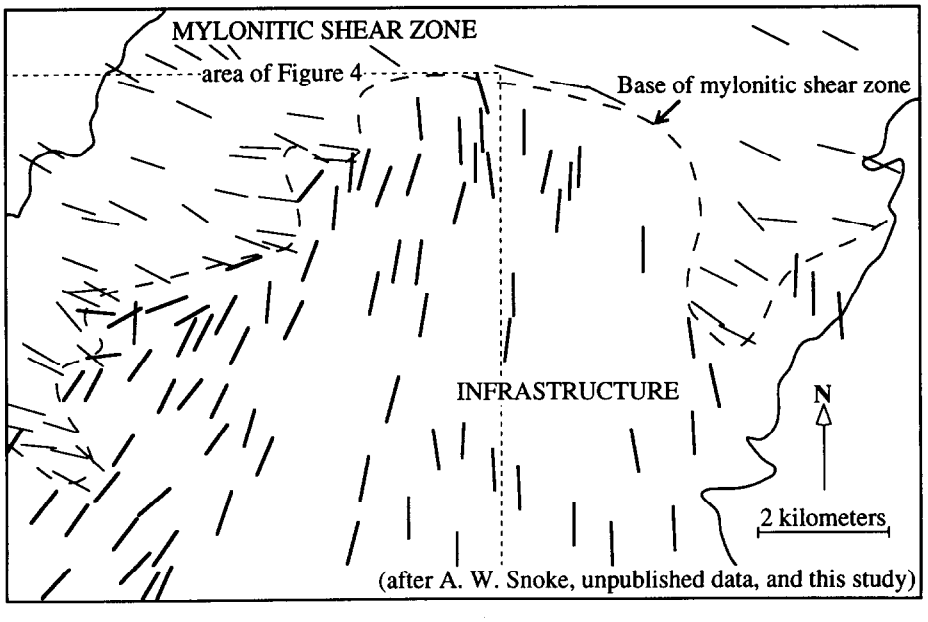

Fig. 2. Lineation trends in the two structural levels of the study area. Thin dashes show lineation trends in the mylonitic shear zone. Thick dashes show trends in the infrastructure. The dashed line marks the change in fabric style from fine-grained mylonites above to coarser infrastructure rocks below.

trending lineation defined by sillimanite needles and feldspar aggregates. The style of deformation in the infrastructure continues to the lowest structural levels exposed in the Ruby Mountains.

The mylonitic shear zone has been described in several previous studies (Howard 1966, Snoke 1980, Snoke & Lush 1984). It is a top-to-the-west–northwest shear zone that roots to the west and has accommodated significant crustal thinning during Oligocene extension. It is known to have been active during the Late Oligocene as several monzogranites dated at 30–29 Ma are strongly mylonitized (Wright & Snoke 1993). Dallmeyer *et al.* (1986) have demonstrated cooling of the area below 300°C by around 25 Ma which puts a younger limit on the age of plastic deformation.

The infrastructure deformation is described in detail by Howard (1966, 1980) and Snoke (1980). Although some of the deformation is probably Mesozoic, MacCready *et al.* (1993) have found the infrastructure lineation and foliation overprinting granitoids dated at 37 and 30 Ma. Thus, the main phase of infrastructure deformation shortly preceded, and may have partially overlapped with, the main phase of mylonitic deformation.

The quartz fabrics preserved in this part of the core complex developed at amphibolite facies conditions at 10–15 km depth. In the mylonitic shear zone Hurlow *et al.* (1991) have determined maximum temperatures of 580–620°C and pressures of 3.1–3.7 kbars. The presence of sillimanite aligned with the lineations in both structural levels indicates amphibolite facies conditions during deformation. The quartz grains within the infrastructure show exaggerated grain growth indicative of amphibolite facies or higher conditions (Wilson 1973). As discussed later, the quartz c-axis patterns are also indicative of these high temperatures.

Quartz c-axis patterns from the infrastructure developed after the main phase of infrastructure flow was complete but while deformation in the mylonitic shear zone was still occurring. The correlation of interpreted temperatures based on the c-axis patterns, and the geothermometry and geochronology results mentioned above, indicate that the quartz textures developed within the period from 30 Ma to 25 Ma. These textures, even within the infrastructure, dominantly reflect the influence of the mylonitic shear zone. They provide insights into the final increments of strain in the core complex which are not recorded in any other minerals.

QUARTZ C-AXIS PATTERNS

Collection of samples

Samples were collected from the Precambrian(?)–Cambrian Prospect Mountain Quartzite. This unit is generally over 95% quartz. During the main phase of infrastructure deformation, the bedding was folded into a series of upright folds and overturned subhorizontal nappes (Howard 1966, 1980, Snoke 1980). These structures were then partially overprinted during the Late Oligocene by the mylonitic shear zone along the west and north edges of the study area. As a result of these geometries it is possible to sample the same unit within both structural levels and also in traverses along continuous layers that span across both the deformation zones. Thus, it is possible to observe how the quartz textures record the transition between the different styles and orientations of deformation in the two zones.

Collection of data

Quartz c-axis orientations were measured on a universal stage. Thin sections were cut perpendicular to foliation and parallel to the elongation lineation visible in hand sample. Thin sections were also cut parallel to foliation to confirm that accessory minerals, primarily sillimanite needles, were indeed parallel to the hand sample lineation. In addition, igneous rocks in the vicinity of each sample contain well developed elongation lineations in the same orientation as in the quartzites. A total of 360 c-axis measurements were obtained for each sample. To ensure a random sampling, measurement points were picked from a standard grid that covered a 1.5×2.0 cm area of each thin section. Non-quartz grains were skipped. When the measurement point lay on the boundary between two quartz grains both were measured. Portions of the thin section that contained excessive ($>10\%$) feldspar or were overprinted by late shear planes were avoided. All measurements made on the quartz grains are included in Fig. 3. Contouring and rotation of the c-axis data was accomplished using the STEREONET 4.4a program developed by R. W. Allmendinger.

Rotation of data

In original plots of the data, most of the patterns are not symmetrical with respect to the elongation lineation. These original plots are shown in column A of Fig. 3. Only in the mylonitic samples do the plots show typical patterns with a strong Y-maximum perpendicular to the lineation (see e.g. RM35, RM57 and RM61 in Fig. 3). In the infrastructure, the c-axes near the foliation are generally not perpendicular to the lineation. On the basis of standard quartz texture interpretation, based on field studies, experiments, and numerical modelling, the c-axes within the foliation should be perpendicular to the flow vector defined by the elongation lineation, i.e. aligned with the Y strain axis (Tullis 1977, Lister & Hobbs 1980, Malaveille & Etchecopar 1981, Schmid & Casey 1986). In addition, the patterns should have a reasonable amount of internal symmetry. Monoclinic or orthorhombic flow should produce patterns with at least a two-fold symmetry axis parallel to the Y strain axis.

Many of the original patterns, shown in column A of Fig. 3, are uninterpretable because they do not have

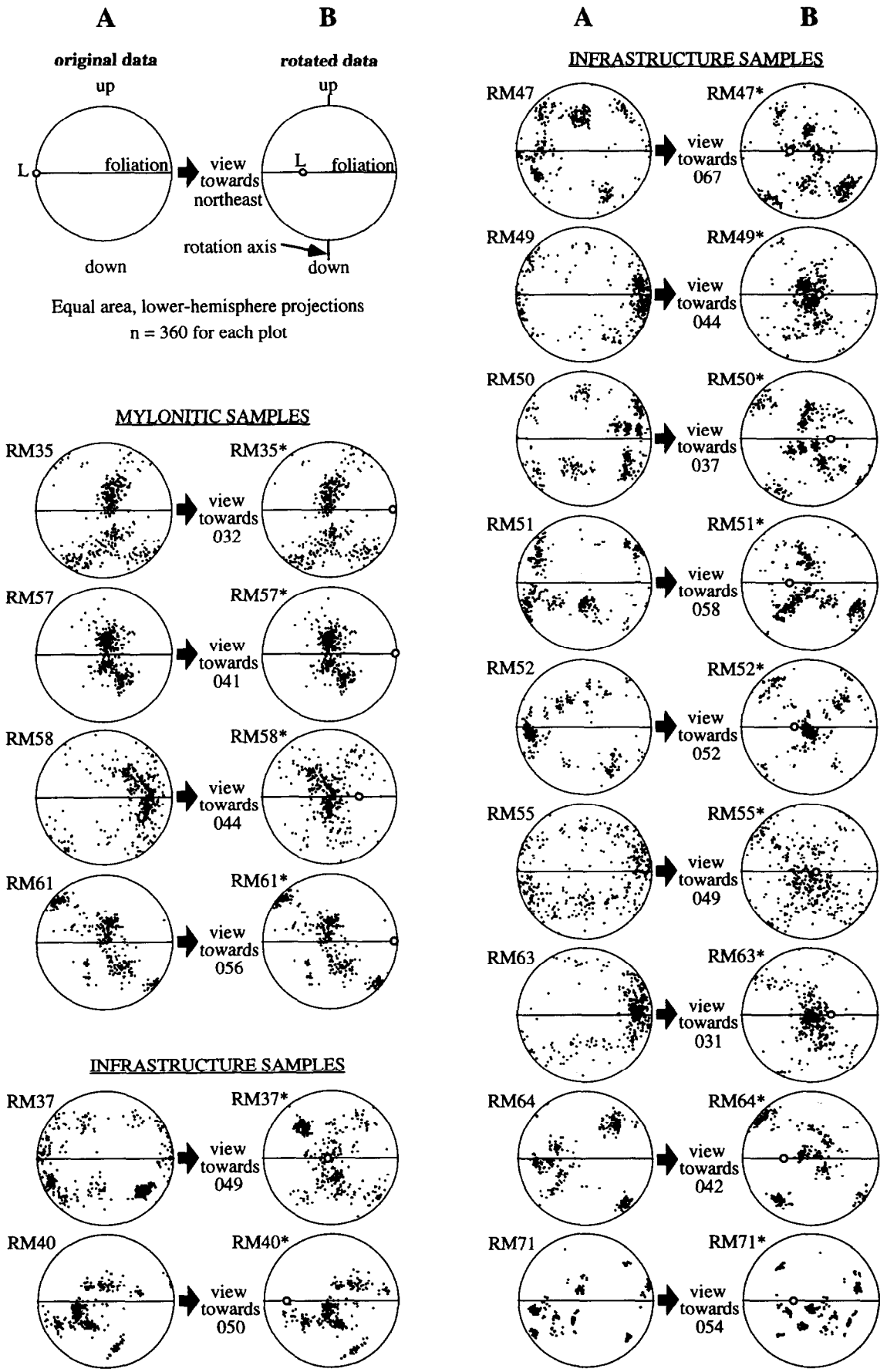

Fig. 3. Stereonet plots of all c-axis data. Column **A** shows the data as originally collected from thin sections cut parallel to the elongation lineation and perpendicular to foliation. Column **B** shows the same data for each sample rotated around the normal to the foliation to bring c-axes in the foliation plane into the center of the stereonet. The resulting lineation orientation is represented by the small, open circle on the foliation plane. The rotated stereonets are all viewed looking northeast.

internal symmetry and are not comparable to typical published patterns. To make the patterns interpretable they were rotated around the normal to the foliation until the main concentration of c-axes within or near the foliation was placed in the center of the stereonet. The amount of rotation is the β value as defined by Simpson (1980) (see technique of Klaper 1988). The rotated patterns, shown in column B of Fig. 3 and denoted with an asterisk (*), look like typical Type I or Type II patterns (Lister 1977). The concentrations of c-axes on or near the foliation plane lie near the center of the stereonet, and the remaining c-axes form either single or crossed girdles.

The rotation is based on the assumption that the foliation was near the slip plane for deformation while the elongation lineation may not necessarily have been in the XZ plane for the incremental strain when the quartz textures developed. Interpretation of the patterns assumes that the rotated patterns are being viewed in this final XZ plane. Ultimately, the new view is justified by the empirical results described below.

(1) There is a regional consistency to the rotated patterns. Figure 4 shows the orientations of the rotated patterns in relation to geographic coordinates. No adjustments were made in this diagram to account for the dip of the foliation plane because the foliations are all subhorizontal (i.e. less than 30° dip). Although each pattern is rotated independently, there is a consistent resulting geographic orientation from one pattern to the next. More importantly, the independently rotated patterns show a more consistent resulting geographic orientation than the elongation lineations (Fig. 5). This regional consistency indicates a regional influence. Thus, the textures developed in the area are not due to a local flow perturbation in each location, but they all appear to have developed in response to a regional strain event.

(2) In most cases the rotated patterns show internal two-fold symmetry. Although the specific concentrations are not evenly distributed within the stereonet, the skeletal outline of each pattern is basically unchanged if the stereonets are rotated 180° in the plane of the page. This level of symmetry is expected when a strain fabric is observed in the XZ plane.

(3) The rotated patterns look like typical patterns observed in nature (e.g. Lister & Dornsiepen 1982, Schmid & Casey 1986, Law *et al.* 1994). Most of the c-axes lie along one or two girdles at an angle to the foliation plane. The patterns are rotated only on the basis of the orientation of c-axes in or near the foliation plane. When near-foliation c-axes are forced into expected positions, the rest of the c-axes end up in expected positions as well.

DISCUSSION

The rotation of the c-axis patterns prior to interpretation is necessary because of the misalignment of the quartz textures and the lineations. The rotation is only a method for achieving an interpretable view of the patterns. By itself it implies nothing about the mechanism that caused the misalignment. This cause must be determined on the basis of regional fabric relations and microfabrics.

The possibility of the quartz textures and infrastructure lineations developing synchronously is ruled out because they exhibit no consistent relations. Although the geographic orientations of the two types of fabric seen in Fig. 5(a) display a conspicuous orthogonal relationship, this is an artifact of the regionally orthogonal overprint of the infrastructure by strain associated with the mylonitic shear zone. Figure 5(b) summarizes the amount that the c-axis patterns needed to be rotated, and it demonstrates the lack of a strong orthogonal correlation for many of the samples. Away from the mylonitic shear zone there is no evidence that the infrastructure lineation has been reoriented by the strain responsible for the quartz crystallographic fabrics.

The misalignment implies that the portion of the strain history responsible for the quartz textures is not equivalent to the portion responsible for the lineation orientations. Although one possibility is that the quartz textures are older, the more consistent geographic orientation of the rotated quartz patterns indicates that the alignment of quartz textures occurred *after* the alignment of lineations. In addition, the quartz textures align with the XZ strain plane in the mylonitic shear zone which generally overprints infrastructure fabrics (Howard 1966, 1980, Snoke 1980).

The geometric results of this study pose the question: how could the quartz textures orient to a new strain direction while the elongation lineations remain unchanged? Both types of fabric are penetrative. Sillimanite needles defining the lineation are often observed entirely within quartz grains that are oriented by the more recent strain. In addition, there is no consistent geographic relation between the quartz texture orientations and the lineation orientations. Thus, it appears that the quartz textures did not reorient through passive rotation of the whole rock fabric. During the late strain event the texture of the quartz has been modified while the rock fabric defined by other minerals has not. This implies that the quartz textures developed by recrystallizing during the late strain event whereas the sillimanite, feldspar and micas were generally unaffected.

Recrystallization mechanisms

The quartz microfabrics reveal a number of recrystallization mechanisms that may have influenced the development of the textures. Figure 6(a) is mylonitic sample RM57 showing grain size reduction. This subgrain development suggests lattice rotation accompanied by rotation recrystallization at high strain rates. Figure 6(b) is sample RM49 from just below the base of the mylonitic shear zone. The ribbon fabric of this quartzite is common in the transition zone between the two structural levels throughout the Ruby Mountains.

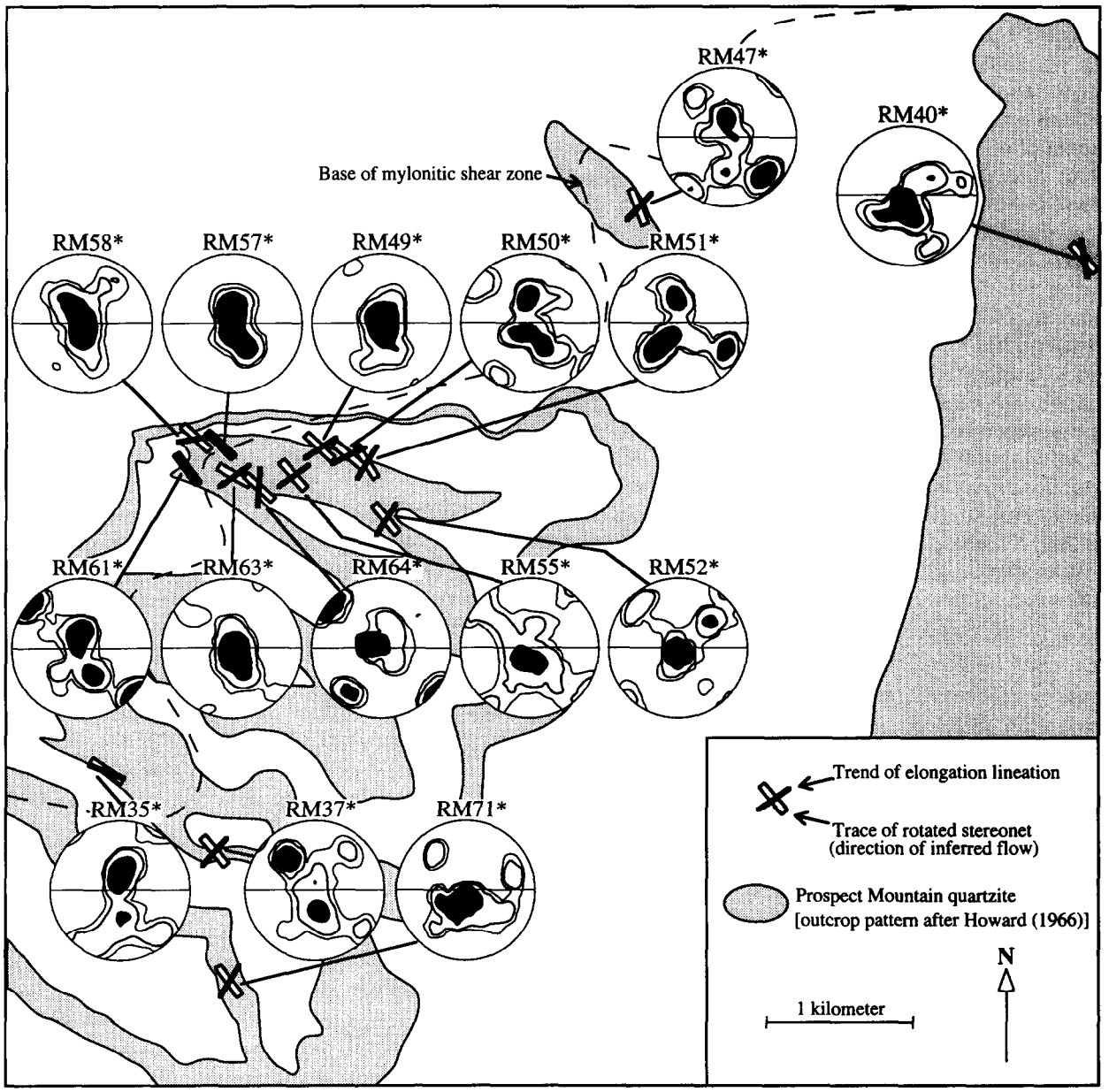

Fig. 4. Contoured, rotated stereonet data showing the location of each sample, the orientations of the rotated stereonets, and the trends of the elongation lineations. The 360 data points for each sample are contoured by the method of Kamb (1959) with contours at 2σ, 4σ, and 10σ (black). The size of the counting circle is 2.4%.

The distortion of the grain shape indicates intracrystalline plasticity which probably produced the lattice rotation. It is interesting to note that, in spite of the difference in fabric style apparent in the photomicrographs, the c-axis patterns from these two samples are remarkably similar (compare RM57* and RM49* in Fig. 4).

Figures 6(c & d) and Fig. 7(a) are infrastructure samples where the large grain size and irregular grain boundaries indicate significant grain boundary migration (GBM). Intracrystalline plasticity must have reoriented some lattices into appropriate orientations during the late strain, as in samples RM57 and RM49, however, complete development of the textures was probably aided by GBM driven to decrease internal strain energy. This style of GBM (as opposed to GBM driven to reduce total surface energy) would tend to eliminate unfavorably oriented grains at the expense of grains appropriately aligned for the late strain increments (Urai *et al.* 1986, Wilson 1986). The question of how deforming grains will orient to accommodate slip, and how dislocation energy will develop in grains based on their orientation, is not yet resolved for quartz deformation (Wenk & Christie 1991). The fact that the infrastructure textures are well developed in regions of significant GBM indicates that grains oriented to accommodate strain on their slip planes did not store as much internal strain energy as grains in other orientations.

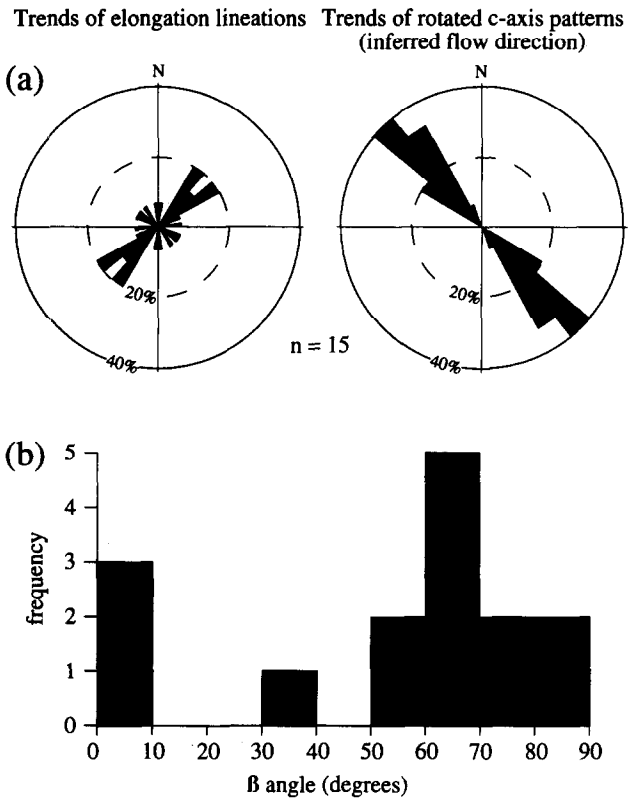

Fig. 5. (a) Rose diagrams summarizing the geographic orientations of lineations (defined by sillimanite and feldspar) and the inferred flow directions based on the quartz crystallographic fabrics. (b) Histogram summarizing the amount of misalignment between the two types of rock fabric (β equals the angle between the perpendicular to the lineation and the c-axes in the foliation plane (Simpson 1980)).

GBM can significantly alter the concentrations of c-axes in a quartzite (Urai *et al.* 1986, Jessell 1988a). Figure 7(b) shows a detail of sample RM61 from the mylonitic shear zone. The evidence for GBM (exaggerated grain growth and pinning of boundaries) in this sample is atypical for the mylonitic rocks. The c-axis pattern for this sample (RM61* in Fig. 4) shows a strong concentration at the margin of the stereonet. Numerical simulations by Jessell (1988b) produce a similar concentration when GBM is included in simulations of simple shear.

An interesting phenomenon in some samples from the Ruby Mountains is the development of interlocking orthogonal grain boundaries. Figures 7(c & d) show details of cross-hatched microstructure development in two of the infrastructure samples. Lister and Dornsiepen (1982) describe similar samples from the Saxony granulite terrain and suggest that these orthogonal grain boundaries develop as microshears. The c-axis patterns for these samples (RM64* and RM51* in Fig. 4) show a tendency to form three roughly orthogonal concentrations. This type of pattern has been studied in detail in high-grade gneisses in Manitoba by Fueten *et al.* (1991). Their study attributes the texture to a stable orientation of intracrystalline shear planes in adjacent quartz domains. It may be that the textures in these two samples from the Ruby Mountains were oriented by a stable combination of internal slip systems and subsequent grain boundary development has mimicked the lattice orientation.

Interpretation of the c-axis patterns

While much of the history of deformation in the Ruby Mountains core complex is found in other fabrics and macroscopic geometries, there is a part of the strain history in the infrastructure that is only recorded by the quartz textures. The Late Eocene to Early Oligocene history of deformation during crustal extension is a separate topic (MacCready *et al.* 1993). The present study is only concerned with the Late Oligocene history of the core complex when the quartz textures developed. The interpretations of strain and temperature discussed below are based on the contoured stereonets shown in Fig. 4.

A transect through samples RM52*, RM55*, RM64*, RM63*, and RM61* shows a relatively smooth change in c-axis patterns from the infrastructure into the mylonitic shear zone. RM52* and RM55* outline Type II crossed girdles that are generally symmetrical. RM64* is similar but is becoming noticeably asymmetric in the number of c-axes in each girdle. RM63*, a transitional sample from just below the base of the mylonitic shear zone, shows the last vestiges of limbs of a second girdle. RM61* is a strongly asymmetric, kinked single girdle.

Two trends are apparent in this transect. First, there is an increase in vorticity of deformation. Whereas the relative symmetry of RM52* and RM55* shows a dominance of pure shear in the infrastructure, the asymmetry of RM61* shows a dominance of simple shear in the mylonitic zone (Platt & Behrmann 1986, Law 1990). The slight asymmetry in other mylonitic samples (e.g. RM57* and RM58*) indicates the same sense of shear. The second trend is the apparent decrease in the temperature of deformation. Samples RM52*, RM55*, and RM64* have consistent opening angles between the girdles of around 85°, similar to upper amphibolite facies patterns (Lister & Dornsiepen 1982). The strong Y-maximum of sample RM63* is typical of amphibolite facies deformation (Jessell & Lister 1990). The spread out girdle of RM61* is typical of greenschist facies deformation (Schmid & Casey 1986). This pattern probably developed later than the other patterns as shear in the mylonitic zone continued to accommodate crustal extension during cooling. It is worth noting that this entire transition in pattern style is comparable to the transition from upper-amphibolite to greenschist facies textures shown in the c-axis patterns of Saxony granulite terrain (Behr 1980, Lister & Dornsiepen 1982).

The rest of the rotated patterns show the same trends mentioned above. Another transect through samples RM51*, RM50*, RM49*, RM57* and RM58* is similar to the first transect. The skeletal outlines of RM47* and RM37* form type I crossed girdles with asymmetric c-axis distributions suggesting a component of top-to-the-west–northwest simple shear close to the mylonitic zone.

Samples RM40* and RM71* produce patterns that significantly deviate from the rest of the region (Fig. 4). In spite of the poor definition of these two patterns, which come from about 1 km below the projected base of the mylonitic shear zone, the rotation technique successfully aligns these patterns with the regional trend.

Implications for footwall strain during crustal extension

Rotated patterns from the infrastructure align with the mylonitic patterns indicating that the infrastructure quartz textures formed under the influence of the same regional strain that produced the mylonitic shear zone. It has been established that the mylonitic shear zone developed during mid-Tertiary crustal extension (Snoke & Lush 1984). Thus, the c-axis patterns of the infrastructure are showing the geometry of this extensional strain beneath the mylonitic shear zone.

The variations in pattern geometry, in particular the changes that indicate the textures formed over a wide range of temperatures, suggest that the quartz textures are recording a temporal change in strain as the core complex cooled. Although the inferred lower temperature c-axis patterns are from samples at higher structural levels, the vertical range of the samples is about one kilometer and it is unlikely that the thermal gradient alone could account for the difference in temperature as the fabrics developed. Earlier strain is preserved in the high temperature infrastructure textures. Here the patterns indicate a dominance of pure shear. Later strain is preserved in textures in and near the mylonitic shear zone, and these indicate a component of simple shear developed during cooling. This temporal change from bulk pure shear to more localized simple shear is similar to the predictions of the penetrative stretching model for crustal extension described by Davis & Hardy (1981) and Miller *et al.* (1983). However, the amount of strain predicted by this model is more than the infrastructure apparently experienced. Another possibility is that the textures may have developed in response to moderate flexure of the footwall during unroofing (Lister & Davis 1989). This may explain why the deepest c-axis patterns, RM40* and RM71*, are less well defined than those higher in the footwall.

When is c-axis pattern rotation appropriate?

The possibility of rotating quartz c-axis patterns has been considered by other workers when faced with patterns that do not show well centered concentrations perpendicular to the elongation lineation (e.g. Klaper 1988, Peterson & Robinson 1993). Klaper (1988), working on the Wandfluhhorn Fold in the Penninic Alps, found a regionally consistent rotated pattern orientation oblique to other lineations but parallel to the larger scale shear direction. GBM was apparently a major factor in the development of these quartz textures at amphibolite facies conditions. Through the analysis of rotated patterns, Klaper (1988) was able to deduce a portion of the strain history that was not found in other minerals. Peterson & Robinson (1993), looking at textures formed at upper amphibolite facies conditions in Massachusetts, examined rotated patterns but chose to interpret the unrotated patterns based on other overprinting relations in the area. Their interpretation thus indicates a major component of <c> slip in producing c-axis concentrations subparallel to the elongation lineation.

Other workers as well, when presented with patterns that do not show a Y-maximum, have chosen to keep their patterns aligned with the elongation lineation and interpret alternative mechanisms for the crystallographic alignment of quartz. In the case of low grade deformation, Stallard & Shelley (1995) demonstrated that quartz may be aligned with c-axes parallel to the stretching direction by grain boundary sliding and mechanical rotation of clastic grains which are naturally elongate parallel to the c-axis. In higher grade areas several workers interpret atypical patterns as indicators of a component of <c> slip active during deformation (Blumenfeld *et al.* 1986, Gapais & Barbarin 1986, Garbutt & Teyssier 1991, Melka *et al.* 1992). Except for the work by Klaper (1988), studies that describe these atypical quartz patterns invoke a different interpretation than the one presented here for the Ruby Mountains. Elevated temperatures have been shown experimentally to be essential for <c> slip to occur (Linker *et al.* 1984). While it is possible that <c> slip is the reason for the atypical patterns, it is also possible that the quartz textures have been reoriented by late strain increments oblique to the lineation. This phenomenon should be suspected whenever the quartz shows abundant evidence for GBM. However, as in this study, when the lineation is no longer considered to be part of the reference frame, some other sort of external confirmation is needed to demonstrate that the rotated view is aligned with the XZ strain plane.

CONCLUSION

Quartz patterns from field studies can only be interpreted by comparison with other published patterns when viewed in the XZ plane of the increments of strain that produced the textures. In most cases this orientation can be determined from the elongation lineation and foliation. When the patterns in this study are viewed in this standard way they are atypical and hence uninterpretable. However, it is possible to determine the appropriate viewing plane by first rotating each pattern until it looks normal and then showing that this new view has a geographically consistent orientation from one pattern to the next. In the absence of a reference frame based on the rock fabric, regional consistency can be used to establish that the quartz has been crystallographically oriented by a regional strain event.

The consistent orientation of the rotated patterns in the Ruby Mountains aligns with normal patterns from a mylonitic shear zone that represents the last stage of

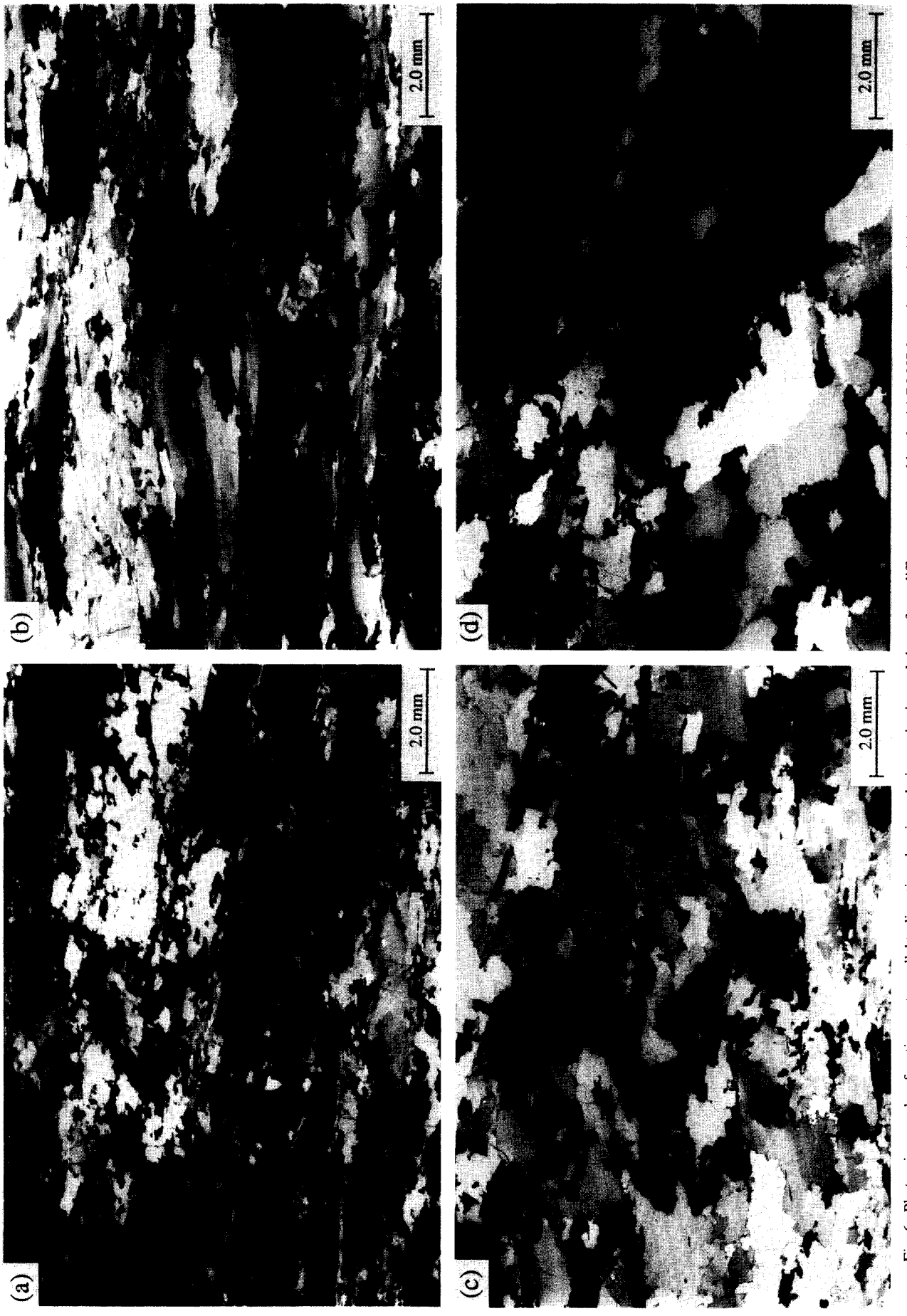

Fig. 6. Photomicrographs of sections cut parallel to lineation showing relative grain size and shape from different structural levels. (a) RM57 from the mylonitic shear zone showing grain size reduction. (b) RM49 from the transitional region 30 m beneath the mylonitic shear zone showing ribbon fabric. (c) RM51 from the infrastructure, 100 m below the mylonitic shear zone, showing exaggerated grain growth. (d) RM40 from 1 km into the infrastructure showing exaggerated grain growth and grain boundary migration.

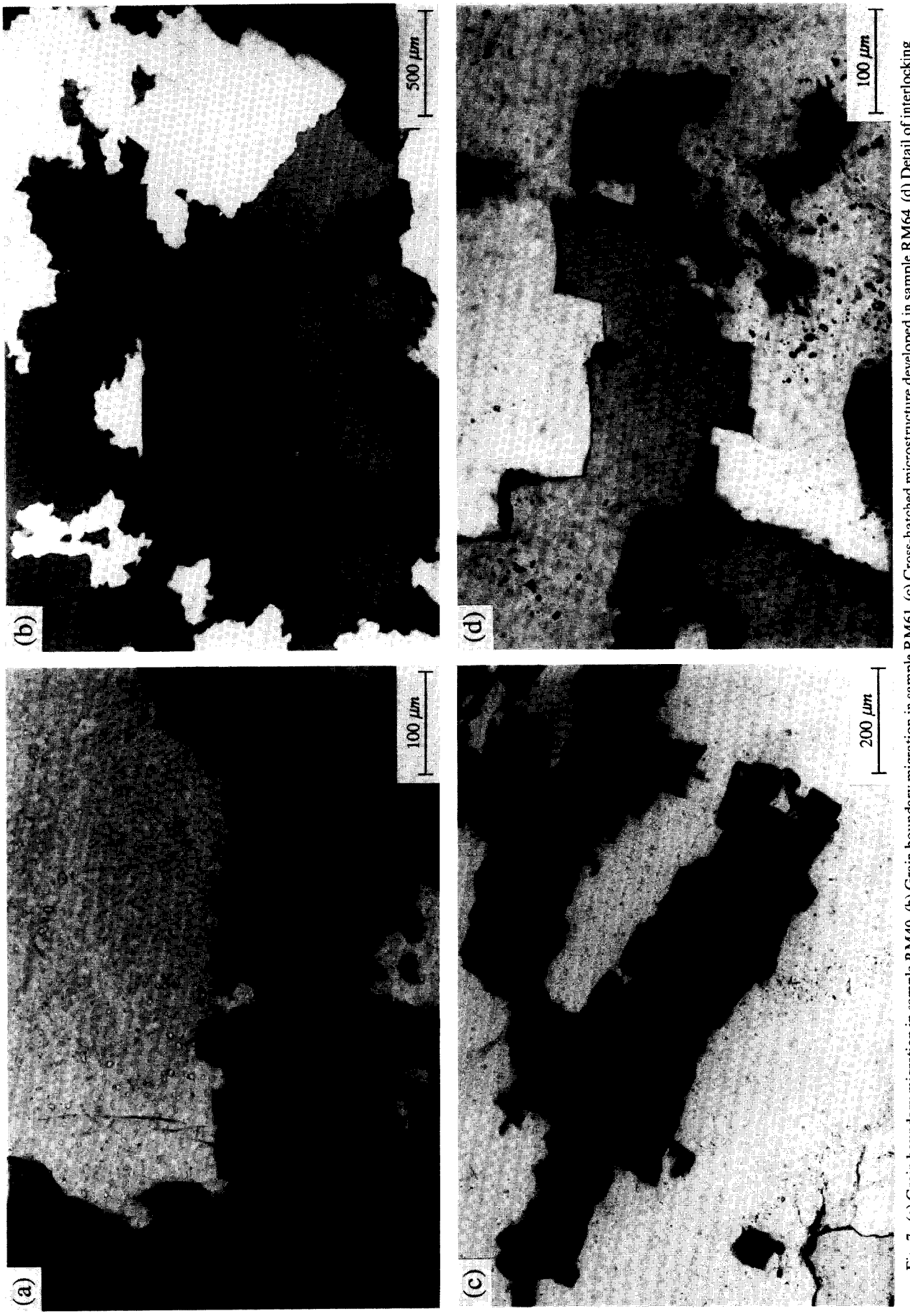

Fig. 7. (a) Grain boundary migration in sample RM40. (b) Grain boundary migration in sample RM61. (c) Cross-hatched microstructure developed in sample RM64. (d) Detail of interlocking grain boundaries in sample RM51.

plastic strain observable in the upper levels of this core complex. Quartz is the only mineral recording late strain outside of the mylonitic shear zone because recrystallization has allowed the quartz textures to readily reorient, whereas sillimanite, feldspar and micas are unaffected. The c-axis patterns indicate that the deeper structural levels of the core complex experienced a small amount of coaxial strain during Late Oligocene crustal extension at amphibolite facies conditions.

Acknowledgements—Art Snoke is thanked for his comprehensive introduction to the structural issues in the Ruby Mountains. The author has benefited from discussions with Mark Jessell, Mark O'Dea and Gordon Lister. Comments on the manuscript by R. D. Law, S. Schmid and H. Stünitz are gratefully acknowledged. This project was funded by a National Science Foundation Graduate Research Fellowship.

REFERENCES

Armstrong, R. L. & Hansen, E. 1966. Cordilleran infrastructure in the eastern Great Basin. *Am. J. Earth Sci.* **264**, 112–127.

Behr, H.-J. 1980. Polyphase shear zones in the granulite belts along the margins of the Bohemian massif. *J. Struct. Geol.* **2**, 249–256.

Blumenfeld, P., Mainprice, D. & Bouchez, J.-L. 1986. C-slip in quartz from subsolidus deformed granite. *Tectonophysics* **127**, 97–115.

Brunel, M. 1980. Quartz fabrics in shear-zone mylonites: evidence for a major imprint due to late strain increments. *Tectonophysics* **64**, T33–T44.

Dallmeyer, R. D., Snoke, A. W. & McKee, E. H. 1986. The Mesozoic–Cenozoic tectonothermal evolution of the Ruby Mountains, East Humboldt Range Nevada: a Cordilleran metamorphic core complex. *Tectonics* **5**, 931–954.

Davis, G. H. & Hardy, J. J. Jr. 1981. The Eagle Pass detachment, southeastern Arizona—Product of mid-Miocene normal faulting in the southern Basin and Range. *Bull. geol. Soc. Am.* **92**, 749–762.

Etchecopar, A. & Vasseur, G. 1987. A 3-D kinematic model of fabric development in polycrystalline aggregates: comparisons with experimental and natural examples. *J. Struct. Geol.* **9**, 705–718.

Fueten, F., Robin, P. F. & Stephens, R. 1991. A model for the development of domainal quartz c-axis fabric in a coarse-grained gneiss. *J. Struct. Geol.* **13**, 1111–1124.

Gapais, D. & Barbarin, B. 1986. Quartz fabric transition in a cooling syntectonic granite (Hermitage massif France). *Tectonophysics* **125**, 357–370.

Garbutt, J. M., Teyssier, C. & 1991. Prism <c> slip in the quartzites of the Oakhurst Mylonite Belt California. *J. Struct. Geol.* **13**, 657–666.

Gleason, G. C., Tullis, J. & Heidelbach, F. 1993. The role of dynamic recrystallization in the development of lattice preferred orientations in experimentally deformed quartz aggregates. *J. Struct. Geol.* **15**, 1145–1168.

Howard, K. A. 1966. Structure of the metamorphic rocks of the northern Ruby Mountains, Nevada. Unpublished Ph.D. thesis, Yale University.

Howard, K. A. 1980. Metamorphic infrastructure in the northern Ruby Mountains, Nevada. In: *Cordilleran Metamorphic Core Complexes* (edited by Crittenden, M. D., Jr., Coney, P. J. & Davis, G. H.). *Geol. Soc. Am. Memoir* **153**, 287–333.

Hurlow, H. A., Snoke, A. W. & Hodges, K. V. 1991. Temperature and pressure of mylonitization in a Tertiary extensional shear zone, Ruby Mountains–East Humboldt Range Nevada: Tectonic implications. *Geology* **19**, 82–86.

Jessell, M. W. 1988a. Simulation of fabric development in recrystallizing aggregates — I. Description of the model. *J. Struct. Geol.* **10**, 771–778.

Jessell, M. W. 1988b. Simulation of fabric development in recrystallizing aggregates — II. Example model runs. *J. Struct. Geol.* **10**, 779–793.

Jessell, M. W. & Lister, G. S. 1990. A simulation of the temperature dependence of quartz fabrics. In: *Deformation Mechanisms, Rheology and Tectonics* (edited by Knipe, R. J. & Rutter, E. H.). *Geol. Soc. Spec. Publ.* **54**, 353–362.

Kamb, W. B. 1959. Ice petrofabric observations from Blue Glacier, Washington, in relation to theory and experiment. *J. geophys. Res.* **64**, 1891–1909.

Klaper, E. M. 1988. Quartz c-axis fabric development and large-scale post-nappe folding (Wandfluhhorn Fold Penninic nappes). *J. Struct. Geol.* **10**, 795–802.

Law, R. D. 1990. Crystallographic fabrics: a selective review of their applications to research in structural geology. In: *Deformation Mechanisms, Rheology and Tectonics* (edited by Knipe, R. J. & Rutter, E. H.). *Geol. Soc. Spec. Publ.* **54**, 335–352.

Law, R. D., Miller, E. L., Little, T. A. & Lee, J. 1994. Extensional origin of ductile fabrics in the Schist Belt, Central Brooks Range, Alaska-II Microstructural and petrofabric evidence. *J. Struct. Geol.* **16**, 919–940.

Linker, M. F., Kirby, S. H., Ord, A. & Christie, J. M. 1984. Effects of compression direction on the plasticity and rheology of hydrolytically weakened synthetic quartz crystals at atmospheric pressure. *J. geophys. Res.* **89**, 4241–4255.

Lister, G. S. 1977. Discussion: crossed-girdle c-axis fabrics in quartzites plastically deformed by plane strain and progressive simple shear. *Tectonophysics* **39**, 51–54.

Lister, G. S. & Davis, G. A. 1989. The origin of metamorphic core complexes and detachment faults formed during Tertiary continental extension in the northern Colorado River region U.S.A. *J. Struct. Geol.* **11**, 65–94.

Lister, G. S. & Dornsiepen, U. F. 1989. Fabric transition in the Saxony granulite terrain. *J. Struct. Geol.* **4 1982**, 81–92.

Lister, G. S. & Hobbs, B. E. 1980. The simulation of fabric development during plastic deformation and its application to quartzite: the influence of deformation history. *J. Struct. Geol.* **2**, 355–370.

Lister, G. S. & Williams, P. F. 1979. Fabric development in shear zones: theoretical controls and observed phenomena. *J. Struct. Geol.* **1**, 283–297.

Lloyd, G. E. & Freeman, B. 1994. Dynamic recrystallization of quartz under greenschist conditions. *J. Struct. Geol.* **16**, 867–881.

MacCready, T., Snoke, A. W. & Wright, J. E. 1993. Evidence for nearly orthogonal, Oligocene crustal flow beneath the coeval mylonitic shear zone of the Ruby Mountains core complex, Nevada. *Geol. Soc. Am. Abs. w. Prog.* **255**, 112.

Malavieille, J. & Etchecopar, A. 1981. Ductile shear deformation of quartzite in an Alpine crustal thrust (Ambin Massif). In: *The Effect of Deformation on Rocks* (edited by Lister, G. S., Behr, H. J., Weber, K. & Zwart, H. J.). *Tectonophysics* **78**, 65–71.

Melka, R., Schulman, K., Schulmannová, B., Hrouda, F. & Lobkowicz, M. 1992. The evolution of perpendicular linear fabrics in synkinematically emplaced tourmaline granite (central Moravia–Bohemian Massif). *J. Struct. Geol.* **14**, 605–620.

Miller, E. L., Gans, P. B. & Garing, J. D. 1983. The Snake Range decollement: an exhumed mid-Tertiary ductile–brittle transition. *Tectonics* **2**, 239–263.

Peterson, V. L. & Robinson, P. 1993. Progressive evolution from uplift to orogen-parallel transport in a Late-Acadian, upper amphibolite- to granulite-facies shear zone, south-central Massachusetts. *Tectonics* **12**, 550–567.

Platt, J. P. & Behrmann, J. H. 1986. Structures and fabrics in a crustal scale shear zone Betic Cordilleras, SE Spain. *J. Struct. Geol.* **8**, 15–34.

Ralser, S., Hobbs, B. E. & Ord, A. 1991. Experimental deformation of a quartz mylonite. *J. Struct. Geol.* **13**, 837–850.

Schmid, S. M. & Casey, M. 1986. Complete fabric analysis of some commonly observed quartz c-axis patterns. In: *Mineral and Rock Deformation: Laboratory Studies — The Paterson Volume* (edited by Hobbs, B. E. & Heard, H. C.). *Am. Geophys. Un. Geophys. Monogr.* **36**, 263–286.

Simpson, C. 1980. Oblique girdle orientation patterns of quartz C-axes from a shear zone in the basement core of the Maggia Nappe Ticino, Switzerland. *J. Struct. Geol.* **2**, 243–247.

Snoke, A. W. 1980. Transition from infrastructure to suprastructure in the northern Ruby Mountains, Nevada. In: *Cordilleran Metamorphic Core Complexes* (edited by Crittenden, M. D., Jr., Coney, P. J. & Davis, G. H.). *Geol. Soc. Am. Memoir* **153**, 287–333.

Snoke, A. W. & Lush, A. P. 1984. Polyphase Mesozoic–Cenozoic deformational history of the northern Ruby Mountains–East Humboldt Range, Nevada. In: *Western Geological Excursions* (edited by Lintz, J., Jr.). *Geol. Soc. Am. 1984 Annual meeting, Reno, Nevada* **4**, 232–260.

Snoke, A. W., McGrew, A. J., Valasek, P. A. & Smithson, S. B. 1990. A crustal cross-section for a terrain of superimposed shortening and

extension: Ruby Mountains–East Humboldt Range metamorphic core complex, Nevada. In: *Exposed Cross-sections of the Continental Crust (NATO ASI Series)* (edited by Salisbury, M. H. & Fountain, D. M.). Kluwer Academic Publishers, Netherlands, 103–135.

Stallard, A. & Shelley, D. 1995. Quartz c-axes parallel to stretching directions in very low-grade metamorphic rocks. *Tectonophysics* **249**, 31–40.

Tullis, J. 1977. Preferred orientation of quartz produced by slip during plane strain. *Tectonophysics* **39**, 87–102.

Urai, J. L., Means, W. D. & Lister, G. S. 1986. Dynamic recrystallisation of minerals. In: *Mineral and Rock Deformation: Laboratory Studies—The Paterson Volume* (edited by Hobbs, B. E. & Heard, H. C.). *Am. Geophys. Un. Geophys. Monogr.* **36**, 161–199.

Wenk, H.-R. & Christie, J. M. 1991. Comments on the interpretation of deformation textures in rocks. *J. Struct. Geol.* **13**, 1091–1110.

Wilson, C. J. L. 1973. The prograde microfabric in a deformed quartzite sequence Mount Isa, Australia. *Tectonophysics* **19**, 39–81.

Wilson, C. J. L. 1986. Deformation-induced recrystallisation of ice: the application of in situ experiments. In: *Mineral and Rock Deformation: Laboratory Studies—The Paterson Volume* (edited by Hobbs, B. E. & Heard, H. C.). *Am. Geophys. Un. Geophys. Monogr.* **36**, 213–232.

Wright, J. E. & Snoke, A. W. 1993. Tertiary magmatism and mylonitization in the Ruby–East Humboldt metamorphic core complex, northeast Nevada: U–Pb geochronology and Sr, Nd, and Pb isotope geochemistry. *Bull. geol. Soc. Am.* **105**, 935–952.